

Equivalent Circuit and Calculation of Its Parameters of Magnetic-Coupled-Resonant Wireless Power Transfer

Hiroshi Hirayama
Nagoya Institute of Technology
Japan

1. Introduction

Because of an improvement of wireless communication technologies, cables are taken away step by step from an electrical equipment. Now, a power cable is the last wire connected to the equipment. Therefore, wireless power transfer (WPT) technology is desired.

Conventionally, microwave power transfer and magnetic induction have been used for this purpose. Microwave power transfer technology utilizes a directivity antenna with high-power microwave generator. This technology is applicable for very long range power transfer, such as space solar power system (SPS). However, this technology requires precise directivity control. Thus it is difficult to use in consumer electrical appliances.

Magnetic induction technology is already used for power supply for a cordless phone, electric tooth brush, or electric shaver. RFID tag also utilizes magnetic induction technology for power supply. However, demerit of this technology is very short distance for power transmission. Although transmitter and receiver is electrically isolated, they should be physically touched. Wireless power transfer using magnetic-coupled resonance is proposed by MIT in 2007 (1). 60W power transmission experiment for 2m distance was demonstrated (2). It is amazing that this technology is applicable although human body is located just between a transmitter and receiver. Thus, it is expected that this technology is used in home electrical appliances or electric vehicles. On the other hands, for practical implementation, design criteria of this system should be established.

Although the magnetic-coupled resonant WPT technology is the epoch-making technology, this technology seems similar technology to magnetic induction. Both of them use magnetic field to transfer power and magnetic coil to feed/pickup power. The key point of the magnetic-coupled resonant WPT is using capacitance to occur resonance. However, even in conventional magnetic induction technology, capacitor is also used. The feature of the magnetic-coupled resonant WPT is to utilize odd-mode and even-mode resonance. In the magnetic induction technology, frequency is fixed according to the transfer distance. However in the magnetic-coupled WPT technology, frequency should be varied according to the transfer distance.

In the section 2, we explain basic theory of magnetic-coupled WPT system through equivalent circuit expression. Method of moment (MoM) simulations will be demonstrated for validation. In the section 3, a procedure to calculate parameters of the equivalent circuit of

magnetic coupled resonant WPT is discussed. Equivalent circuit parameters are calculated from the geometrical and material parameters of the WPT structure. Radiation loss and conductive loss are taken into account in the equivalent circuit. Both direct-fed type and indirect-fed type structures are considered. MoM calculation shows that the equivalent circuit has capability to calculate S parameters and far-field radiation power correctly.

2. Basic theory of magnetic-coupled resonant WPT system

2.1 Classification of coupled resonant WPT system

The coupled resonant WPT system is classified from the viewpoint of 1) field used in coupling, 2) power feeding, and 3) resonant scheme.

From the viewpoint of field, this system is classified to magnetic-coupled resonant type and electric-coupled resonant type. Not only magnetic field but also electric field can be used for coupled-resonant WPT. In the case of magnetic-field coupling, power transfer is affected by surrounding permeability. On the other hand, for electric-field coupling, power transfer is affected by surrounding permittivity. Because the relative permeability of human body is almost unity, magnetic-coupled resonant WPT is not affected by human body. Therefore, magnetic-coupled type is used in the reference (2). However, when the effect of a human body is negligible, electric-field coupling type may be a considerable alternative.

From the viewpoint of power feeding, this system is classified to direct fed type and indirect fed type. In the case of the direct fed type, power source and load is directly connected to the resonant structure. On the other hand, feeding loop is used for indirect fed type. A power source and load is connected to the loop structures, which have not sharp frequency characteristics. The loop structure and the resonant structure is coupled by magnetic induction. A merit of direct fed type is simple structure. On the other hand, indirect type has advantage in freedom of design: impedance matching is achieved by adjusting the spacing between the loop and the resonant structure.

From the viewpoint of resonant scheme, this system is classified to self resonant type and external resonant type. To occur resonance, same quantity of inductive reactance and capacitive reactance is necessary. For the self resonant type, inductance and capacitance are realized by identical structure. For example, open-end spiral structure is used. Currents along the spiral structure causes inductance and charges at the end of the spiral causes capacitance. Resonant occurs at the frequency at which the inductive and the capacitive reactance becomes same. On the other hands, external resonant type has distinct structure to realize capacitance and to realize inductance. For example, loop structure is used for inductance and discrete capacitor is added for capacitance.

In accordance with the above discussed classification, the WPT system shown by MIT (2) is magnetic-coupled resonant, indirect-fed, self resonant type.

Although this system is regarded to be a new technology, its principle can be discussed from following standpoints. 1) this system is a TX antenna and a RX antenna. 2) this system is two element TX array antenna which has parasitic element terminated with a resistor. 3) this system is coupled resonators. 4) this system is a transformer with capacitors. The viewpoint 1) is useful to discuss impedance matching or power transfer efficiency. However, since this system is used in near-field region, a concept based on far-field region, such as gain or directivity, is not applicable. The viewpoint 2) is beneficial to consider far-field emission or interaction between TX and RX antenna. From a viewpoint of electro-magnetic

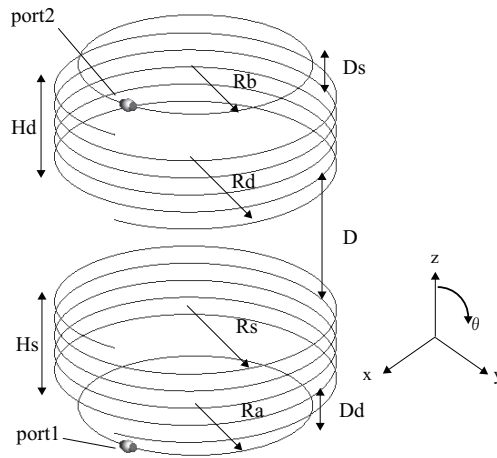


Fig. 1. Calculation model

	D_s	D	D_d	H_s	H_d	R_a	R_b	R_s	R_d
[mm]	50	300	50	200	200	250	250	300	300

Table 1. Parameters of the calculation model

resonant mode, the viewpoint 3) provides considerable knowledge, as in the reference (2). The viewpoint 4) is profitable to predict input impedance or resonant frequency from an equivalent circuit. On the other hands, this is unsuitable to discuss undesired emission or effect to human bodies from a viewpoint of electromagnetics. In this section, we unveil mechanism of power transfer from a suitable standpoint.

2.2 Investigation on resonant mechanism

A consideration model is shown in Fig. 1. Structural parameters are listed in Table 1. This model is used in the reference (2), which is classified magnetic-coupled resonant, indirect-fed, self resonant type. The loop structure is used to feed. The helical structure is used to occur resonance. The loop structure and the helical structure is coupled by magnetic inductance. The helices are coupled by magnetic-coupled resonance.

This structure is analyzed by MoM calculation. Perfect electric conductor (PEC) is assumed in this calculation. Figure 2(a) shows input impedance. The case without helix is also plotted. By using the helix, two resonances are occurred.

Figure 2(b) shows real part and imaginary part of the port current. Port 1 is input port and Port 2 is output port. We can see that at the lower frequency resonance, input port and output port have same polarity of current. On the other hand, at the higher frequency resonance, input port and output port have opposite polarity of current.

Magnetic field distributions at these frequencies are shown in Fig. 3 and 4. Sub-figure (a) shows magnitude of magnetic field vector, (b) shows z-direction component of magnetic field vector, which corresponds to vertical direction in the figure, and (c) shows y-direction component, which corresponds to horizontal direction in the figure. At the lower frequency

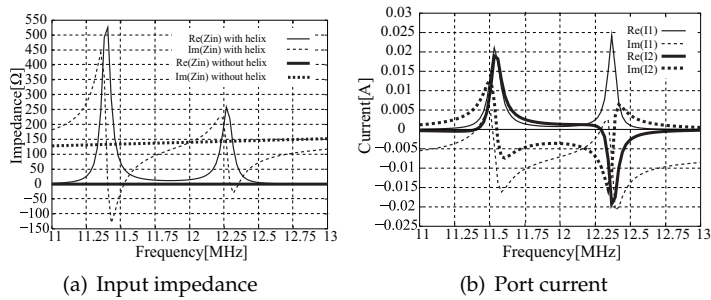


Fig. 2. Frequency characteristics of the consideration model

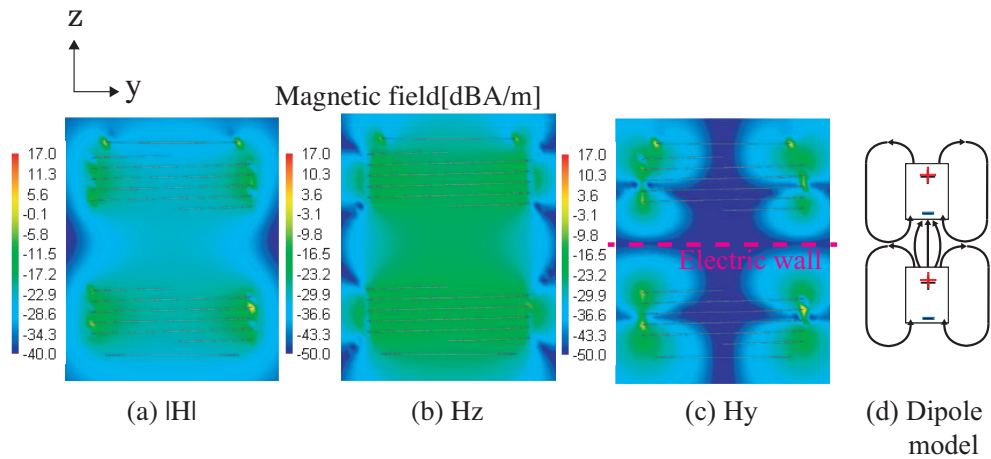


Fig. 3. Magnetic field distribution on a frequency of the odd mode(11.4MHz) and equivalent dipole model

resonance, there is no y component magnetic field at the center of TX and RX. Therefore electric wall is located between TX and RX. Considering the polarity of port current, this resonant mode is modeled by magnetic dipole shown in sub-figure(d). Since the magnetic charge distribution along z axis is asymmetrical, this resonant mode can be called odd mode. On the other hand, at the higher frequency resonance, there is no z component magnetic field at the center of TX and RX. Therefore magnetic wall is located between TX and RX. Since the magnetic charge for this frequency is symmetrical, this resonant mode can be called even mode.

Next, let us see power transmission efficiency. Power transmission efficiency is defined by

$$\eta = \frac{Z_l |I_2|^2}{|I_1| |V_1|} \tag{1}$$

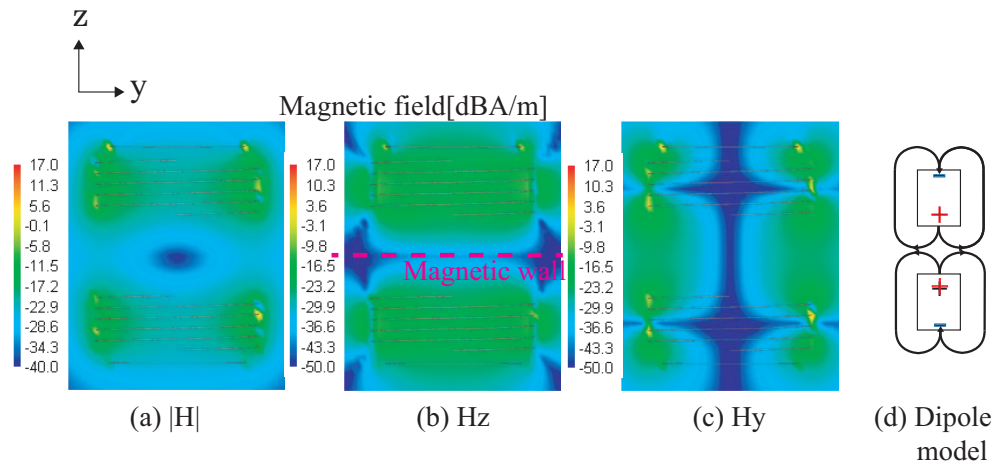


Fig. 4. Magnetic field distribution on a frequency of the even mode(12.3MHz) and equivalent dipole mode

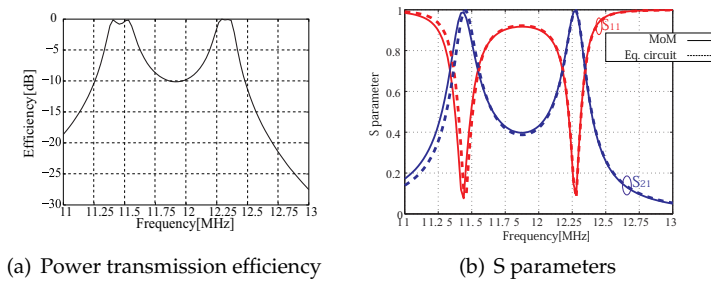


Fig. 5. Frequency characteristics of the transmission specifications

Figure 5(a) shows the calculated result. There are two peaks of efficiency both for odd and even mode. The imaginary part of the input impedance (Fig. 2(a)) is not zero at the frequency of resonance since the input impedance includes the inductance of the loop structure. Therefore, the resonant frequency and the frequency at which the input impedance becomes zero become different. From the viewpoint of power engineering, this definition means effective power of the output port normalized by apparent power of the input port. It is said that the power transmission efficiency is maximized when the power factor becomes unity. From the viewpoint of radio frequency engineering, S parameter is important index. Figure 5(b) shows calculated S parameters. At the odd and even mode frequencies, S_{21} becomes almost unity.

We assume a sphere which surrounds the transmitting and receiving antenna. By applying the Poynting theorem to the volume of the sphere V and the surface of the sphere S , a balance of the power is described as

$$P_p = P_r + P_w + P_d \tag{2}$$

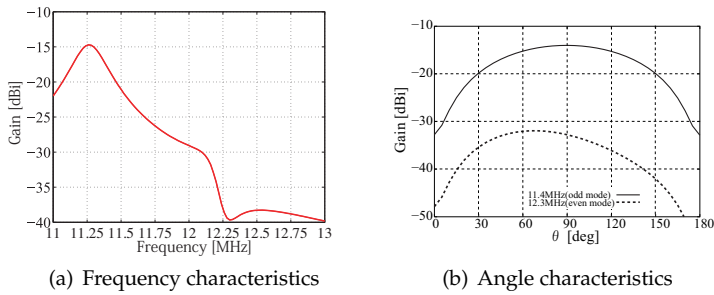


Fig. 6. Gain as transmitting antenna

where

$$P_p = \iiint_V P_s dV \tag{3}$$

$$= P_{in} - P_{out} \tag{4}$$

$$P_r = \iint_S \mathbf{S} \cdot \mathbf{n} dS \tag{5}$$

$$P_w = \frac{\partial}{\partial t} \iiint_V \left(\frac{1}{2} \mu \mathbf{H}^2 + \frac{1}{2} \epsilon \mathbf{E}^2 \right) dV \tag{6}$$

$$P_d = \iiint_V \sigma \mathbf{E}^2 dV \tag{7}$$

and P_{in} is a power supplied to the port of the transmitting antenna, P_{out} is a power extracted from the port of the receiving antenna, P_r is a power of far-field emission, P_w is stored energy in the volume V , and P_d is loss power dissipated in the volume V . For an antenna used for far-field, an antenna is a device which transduces P_p into P_r . However, since the wireless power transmission is a system which extracts P_{out} from the P_{in} , P_r becomes a loss energy.

An antenna used in far-field is required to maximize far-field emission, i.e. to maximize a gain. In the wireless power transmission, far-field emission becomes not only power loss but also a cause of electro-magnetic interference (EMI). Thus, reducing far-field emission is required. The far-field emission can be estimated from the gain by regarding this system as an array antenna consisted of the TX antenna and the RX antenna. In this calculation, RX antenna is considered as a parasitic element loaded with a loss resistance located in the vicinity of the TX antenna. Fig. 6(a) shows the gain as antenna for x direction. Fig. 6(b) shows angle specifications of gain for the odd and the even mode frequencies. The maximum gain was -13.8 dBi and -31.8 dBi for odd and even mode, respectively. The gain of the even mode frequency for the maximum emission direction is smaller by 18 dB than that of the odd mode frequency.

Strength of undesired emission is specified by using effective isotropic radiation power (EIRP):

$$EIRP = G_t P_t \tag{8}$$

where G_t and P_t show gain of antenna shows power fed to the antenna, respectively. EIRP for the 1W power transfer is 41.7mW for odd mode and 0.66mW for even mode. Since the current of the TX antenna and RX antenna has opposite direction for the even mode, the resultant

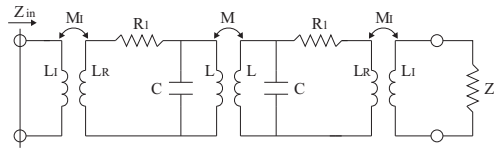


Fig. 7. Equivalent circuit model

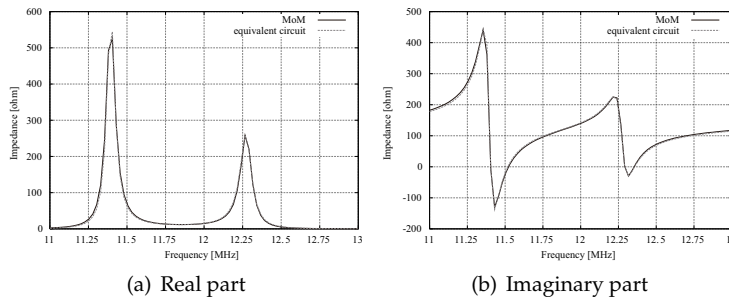


Fig. 8. Input impedance calculated by MoM and the equivalent circuit model

emission from the TX and RX antennas is canceled each other in far field. This result shows that the even mode is suitable for use because of low undesired radiation.

2.3 Investigation on resonant frequency with equivalent circuit model

Equivalent circuit of the wireless power transmission is shown in Fig. 7. L , C , and M represent self inductance of the helix structure, stray capacitance of the helix structure, and the mutual inductance between transmitting and receiving helices, respectively. R_I and Z_I represent loss resistance of the helix structure and load impedance, respectively. L_r and L_I correspond to self inductance of the induction coil and self inductance of the helix which concerns with the coupling to the induction coil, respectively. M_I shows the mutual inductance between induction coil and resonant helix. Figure 8(a) and 8(b) show input impedance calculated by the MoM and the equivalent circuit, respectively. We can see that the physical phenomenon of WPT is adequately represented by the equivalent circuit.

Because the loop structure does not concern with a resonant mechanism, resonant frequency determined by the L , M , and C will be considered. Resonant frequency of the helical structure f_0 becomes

$$f_0 = \frac{1}{2\pi\sqrt{LC}} \tag{9}$$

When two helices are coupled each other, odd mode resonance and even mode resonance occur. Resonant frequency of odd mode and even mode, f_{odd} and f_{even} , becomes as follows:

$$f_{\text{odd}} = \frac{1}{2\pi\sqrt{C(L+M)}} \tag{10}$$

$$f_{\text{even}} = \frac{1}{2\pi\sqrt{C(L-M)}} \tag{11}$$

In the case of odd mode resonant, because polarity of current of the TX and the RX coil is same, mutual inductance is added to the mutual inductance. Thus, f_{rmodd} becomes smaller than f_0 . In the case of even mode resonant, because polarity of current of the TX and the RX coil is opposite, mutual inductance is substituted from the mutual inductance. Thus, f_{rmodd} becomes higher than f_0 .

Coupling coefficient k is defined by

$$k = \frac{M}{L}, \quad (12)$$

which shows strength of coupling between the TX and the RX loop. By using the k , the odd and the even mode resonant frequency is obtained by

$$f_{\text{odd}} = \frac{f_0}{\sqrt{1+k}} \quad (13)$$

$$f_{\text{even}} = \frac{f_0}{\sqrt{1-k}}. \quad (14)$$

For the traditional WPT system using magnetic induction, frequency is fixed with respect to the distance between TX and RX. However, for the magnetic-coupled resonant WPT system, resonant frequency varies with respect to the distance between TX and RX. In the practical use, available frequency is determined due to regulation. To maintain resonant frequency, capacitance should be adaptively changed.

f_0 and k is obtained when the resonant frequency of the odd and the even mode is known:

$$f_0 = \sqrt{\frac{2f_{\text{even}}^2 f_{\text{odd}}^2}{f_{\text{even}}^2 + f_{\text{odd}}^2}} \quad (15)$$

$$k = \frac{f_{\text{even}}^2 - f_{\text{odd}}^2}{f_{\text{even}}^2 + f_{\text{odd}}^2}. \quad (16)$$

To estimate f_0 and k from an experimental result, this equations can be used.

3. Calculation of equivalent circuit parameters

3.1 Consideration model

Fig. 9 shows a structure of the direct-fed type wireless power transfer. Both transmitting (TX) and receiving (RX) antennas consist of one-turn loop whose radius is r . The circumference of the loop is assumed to be much smaller than the wavelength of the operating frequency. The loops are made of wire whose diameter is $2d$ and conductivity is σ . Distance between TX and RX is h . Capacitor C_0 is connected to occur resonance.

Equivalent circuit of this structure is shown in Fig. 10. Z_S and Z_L show source impedance and load impedance, respectively. L and M show self and mutual inductance of the loops, respectively. R_r and R_l show radiation resistance and conductive loss resistance, respectively. Fig. 11 shows a consideration model of the indirect-fed type. Loops 1 and 2 are for TX, and 3 and 4 are for RX. Loops 1 and 4 are feeding coils, which are connected to the power source and the load, respectively. Loops 2 and 3 are resonant coils, to which the resonant capacitors

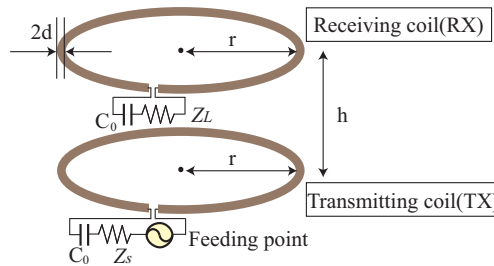


Fig. 9. Consideration model of direct-fed type WPT structure

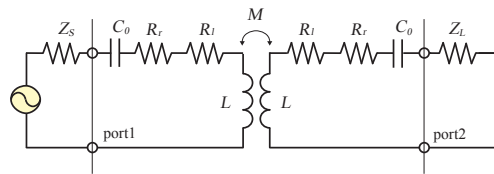


Fig. 10. Equivalent circuit of the direct-fed model

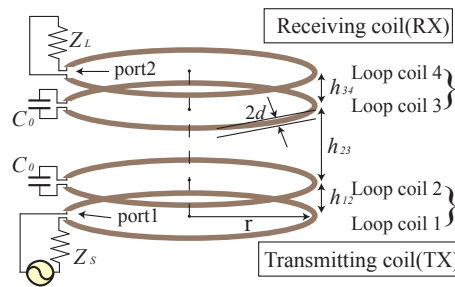


Fig. 11. Consideration model of indirect-fed type WPT structure

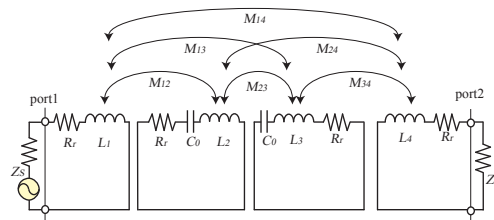


Fig. 12. Equivalent circuit of the indirect-fed model

are connected. Power is transferred by magnetic induction between the feeding coil and the resonant coil. Between resonant loops, power is transferred by magnetic coupled resonant. This WPT system is characterized by the geometrical dimensions: loop radius r , radius of wire d , distance between loops h_{12} , h_{23} , and h_{34} .

Equivalent circuit of this structure is shown in Fig. 12. L_i shows self inductance of i -th loop. M_{ij} shows mutual inductance between i -th and j -th loops. In this consideration, all combination of mutual coupling is considered. Equivalent circuit parameters are calculated in the same manner as the direct-fed type.

3.2 Equivalent circuit parameters

By using the Neumann's formula, mutual inductance M becomes

$$M = \frac{\mu_0}{4\pi} \oint_{l_1} \oint_{l_2} \frac{d\vec{l}_1 \cdot d\vec{l}_2}{r_{12}} \quad (17)$$

where μ_0 shows permeability of free space, dl_1 and dl_2 show line element of TX and RX loops, respectively, and r_{12} shows distance between dl_1 and dl_2 . Assuming that two loops are arranged as shown in Fig. 9, M is reduced to

$$M = \mu_0 \sqrt{r_1 r_2} \left\{ \left(\frac{2}{k} - k \right) K(k) - \frac{2}{k} E(k) \right\} \quad (18)$$

$$(19)$$

where

$$k = \frac{4r_1 r_2}{(r_1 + r_2)^2 + h^2}$$

and $K(k)$ and $E(k)$ are complete elliptic integrals:

$$K(k) = \int_0^{\pi/2} \frac{1}{\sqrt{1 - k^2 \sin^2 \phi}} d\phi \quad (20)$$

$$E(k) = \int_0^{\pi/2} \sqrt{1 - k^2 \sin^2 \phi} d\phi. \quad (21)$$

Self inductance L is calculated from external inductance L_e and internal inductance L_i :

$$L = L_e + L_i \quad (22)$$

The external inductance is due to magnetic field caused around the conductor. Assuming that all the current I is concentrated along the center line C shown in Fig. 13, resultant magnetic flux inside the C is identical to that inside the C' . Thus, by substituting $r_1 = r$, $r_2 = r - d$, $h = 0$ into the Eq. (18), L_e is calculated. Eq. (18) is approximated to

$$L_e \approx \mu_0 r \left(\ln \frac{8r}{d} - 2 \right) \quad (23)$$

assuming $r_1 \approx r_2$, $h \ll r_1, r_2$.

The internal inductance is caused by magnetic fields in the conductor. If the loop is perfect conductor, currents flow only on the surface of the conductor, then internal inductance is

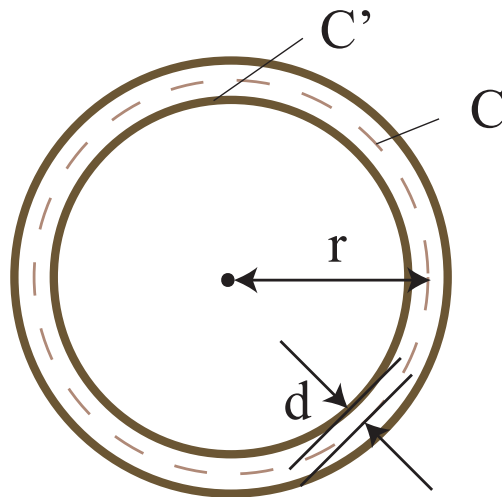


Fig. 13. External inductance L_e

negligible. Considering the conductivity, skin depth δ is calculated from

$$\delta = \frac{1}{\sqrt{\omega\mu\sigma}}. \quad (24)$$

Internal inductance becomes

$$L_i = \frac{\Phi_i}{I} = 2\pi r \frac{\int_{d-\delta}^d B_i dr'}{I} \quad (25)$$

where I , Φ_i , B_i and μ show current in the conductor, flux linkage, flux density in the conductor, permeability of the conductor, respectively. B_i is obtained from Ampere's law:

$$B_i = \mu \frac{NI}{2\pi r'} \quad (26)$$

where $r' (d - \delta < r' < d)$ shows distance from the center of the conductor. Current density in the conductor becomes uniform assuming $\delta > d$, thus internal inductance becomes

$$L_i = \frac{\mu r}{4}. \quad (27)$$

Because the circumference is much smaller than the wavelength, radiation resistance R_r is approximated to

$$R_r = 20\pi^2(\beta r)^4 \quad (28)$$

where $\beta = 2\pi/\lambda$.

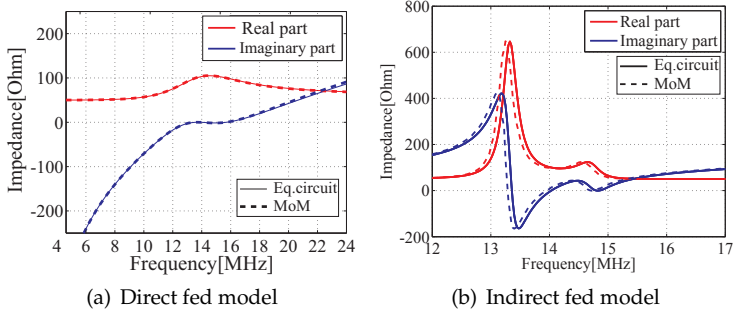


Fig. 14. Input impedance

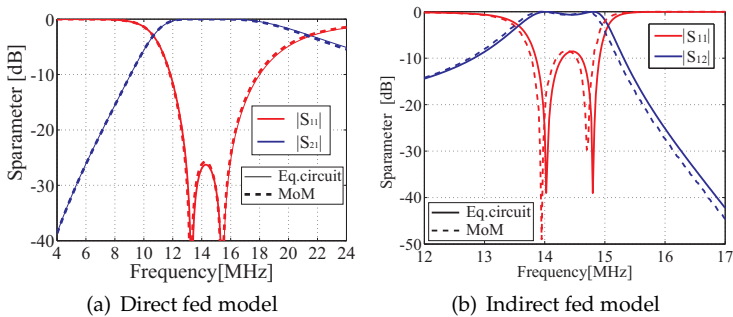


Fig. 15. S parameters

Taking the skin effect into account, conductive loss is obtained by

$$R_l = \frac{2\pi r}{\sigma \cdot S} \tag{29}$$

where $S = \pi\{d^2 - (d - \delta)^2\}$ is cross section in which current flows. Finally, resonant capacitance becomes

$$C_0 = \frac{1}{(2\pi f_0)^2 L} \tag{30}$$

3.3 Numerical validation

To discuss adequateness of the equivalent circuit, input impedance and S parameters calculated by the proposed procedure are compared with those calculated by MoM. Geometrical dimensions are set to be $r = 20\text{cm}$, $d = 1\text{mm}$, and $h = 2\text{cm}$. Resonant frequency is designed to be 13.2MHz. Figure 14(a) shows the real part and the imaginary part of the input impedance. Figure 15(a) shows frequency characteristics of S parameters. From the S_{11} , two resonant modes, that is odd mode and even mode, are confirmed. It is proved that the procedure to calculate equivalent circuit parameters is adequate.

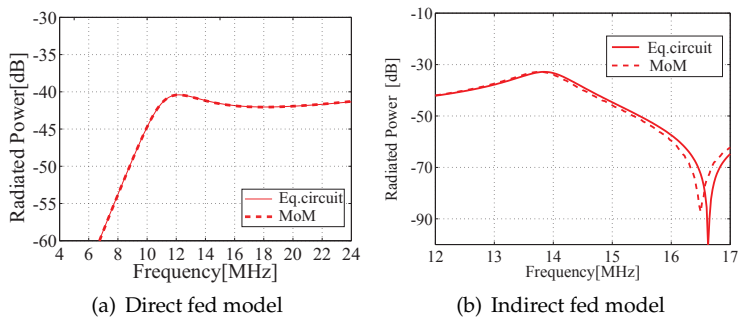


Fig. 16. Far field radiation power

In the case of the indirect-fed model, input impedance and S parameters are calculated through impedance matrix \mathbf{Z} :

$$\mathbf{Z} = j\omega\mathbf{Z}_I + \mathbf{Z}_E + \mathbf{Z}_R \tag{31}$$

where

$$\mathbf{Z}_I = \begin{bmatrix} L_1 & M_{12} & M_{13} & M_{14} \\ M_{12} & L_2 & M_{23} & M_{24} \\ M_{13} & M_{23} & L_3 & M_{34} \\ M_{14} & M_{24} & M_{34} & L_4 \end{bmatrix} \tag{32}$$

$$\mathbf{Z}_E = \text{diag} \left(Z_S, \frac{1}{j\omega C_0}, \frac{1}{j\omega C_0}, Z_L \right) \tag{33}$$

$$\mathbf{Z}_R = (R_L + R_r)\mathbf{I}. \tag{34}$$

and $\text{diag}(\cdot)$ and \mathbf{I} show diagonal matrix and identity matrix, respectively.

Far-field radiation power is calculated from

$$P_r = \frac{1}{2} \left(R_r |I_1 + I_2 + I_3 + I_4|^2 \right). \tag{35}$$

Figure 14(b) and 15(b) shows calculation result. MoM result almost agreed with the result of the equivalent circuit. However, in comparison with the direct-fed type, error can be seen. In the case of the indirect-fed type, the feeding loop is closed to the resonant loop. It is considered that this error is caused by stray capacitance between feeding loop and resonant loop.

In the equivalent circuit, total power dissipated in the radiation resistance becomes

$$P_r = \frac{1}{2} \left(R_r |I_1|^2 + R_r |I_2|^2 \right). \tag{36}$$

However, far-field radiation due to TX and RX loops is added in field strength, not in power. Thus, radiation power P_r is calculated considering phase of current:

$$P_r = \frac{1}{2} \left(R_r |I_1 + I_2|^2 \right). \tag{37}$$

Figure 16(a) and 16(b) shows calculated result. In this graph, power is normalized by the incident power to the port 1. It is shown that the proposed procedure has a capability to estimate far-field radiation power correctly.

Figure 17 shows dependency of S parameters on distance of transmitting at the resonant frequency. It is confirmed that the equivalent circuit represent S parameters correctly.

Figure 18 shows effect of conductivity on S parameters. It is shown that conductivity of material is adequately taken account in the equivalent circuit.

To discuss the limitation of the equivalent circuit, we calculated S parameters with respect to the radius of the loop. Figure 19 shows S parameter of radius 10cm($2\pi r=0.0276\lambda$), 30cm($2\pi r=0.0830\lambda$), 40cm($2\pi r=0.1106\lambda$), 50cm($2\pi r=0.1382\lambda$). When the radius of the loop becomes larger, the MoM result is not in accordance with the result of the equivalent circuit. It is considered that when the loop becomes large, circumference is not negligible compared to the wavelength then current distribution on the coil becomes not uniform.

3.4 Experimental validation

To validate simulation result, experimental model was fabricated. Figure 20(a) shows configuration of the experimental model. Copper wire and 100pF ceramic capacitors were used.

Measured S parameters using VNA are shown in Fig.20(b). S parameters obtained by the equivalent circuit are also plotted. For the equivalent circuit, conductivity is fit to consistent with the experimental value. Conductivity of $1.90 \times 10^4 [1/\Omega \cdot m]$ gave most suitable S

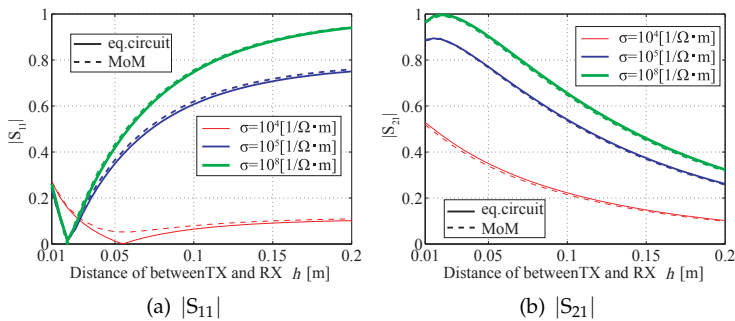


Fig. 17. Effect of transfer distance on the S parameters

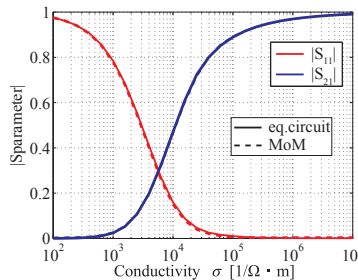


Fig. 18. Effect of the conductivity on the S parameters

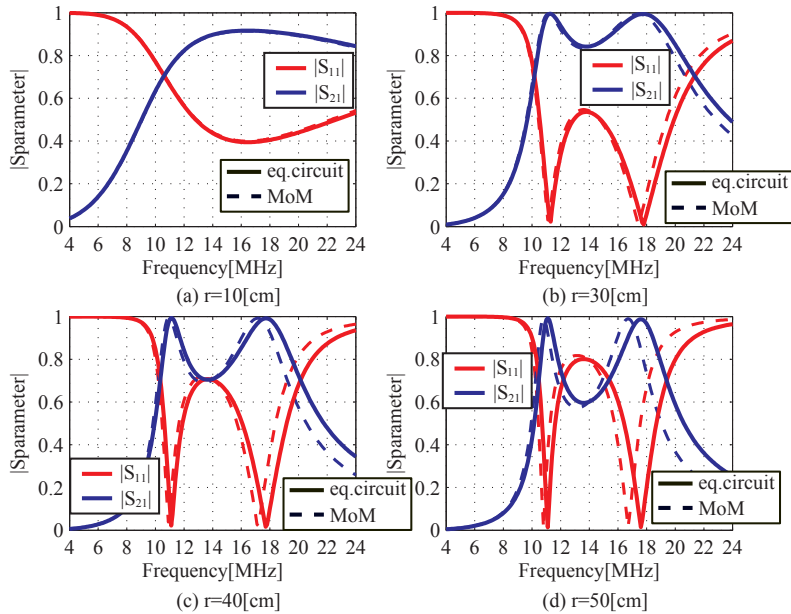


Fig. 19. Frequency characteristics of the S parameters ($\sigma = 10^8 [1/m \cdot \Omega]$, $h = r/16$)

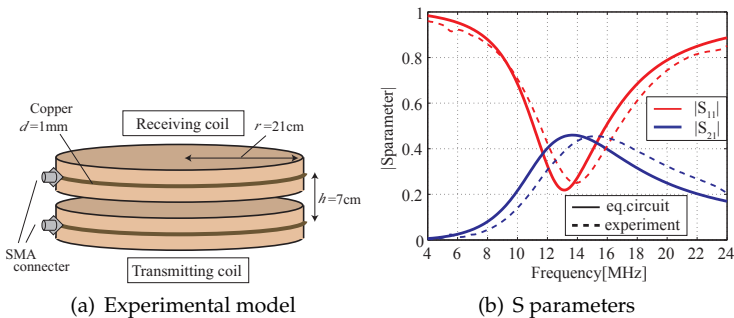


Fig. 20. Experimental validation

parameters for the experimental result whereas literature value is $6.80 \times 10^7 [1/m \cdot \Omega]$. It is considered that a cause of the error is dielectric loss of the capacitor.

4. Conclusion

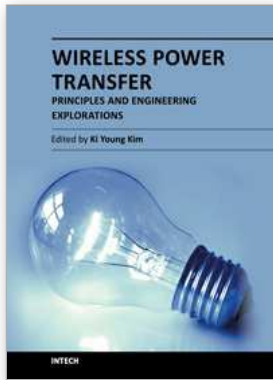
In this chapter, resonant mechanism of magnetic-coupled resonant wireless power transfer was demonstrated. There are odd mode and resonant mode resonance. In the odd mode resonance, port current of input port and output port are opposite polarity. Electric wall is formed between TX and RX. Resonant frequency becomes lower because total inductance becomes self inductance plus mutual inductance. Since far-field radiation from TX and RX

are in-phase, undesired emission becomes large. In the even mode resonance, port current of input port and output port are same polarity. Magnetic wall is formed between TX and RX. Resonant frequency becomes higher because total inductance becomes self inductance minus mutual inductance. Since far-field radiation from TX and RX are out-of-phase, undesired emission becomes small. From the viewpoint of low undesired emission, even mode resonant is better to use.

Next, equivalent circuit of WPT system and procedure to calculate its parameters from geometrical dimensions was shown. Both radiation loss and conductive loss are taken into account in the equivalent circuit. MoM calculation shows that the equivalent circuit has capability to calculate S parameters and far-field radiation power correctly. It is expected to utilize the equivalent circuit to design a matching network.

5. References

- [1] Andre Kurs, Arsteidis Karalis, Robert Moffatt, John Joannopoulos, Peter Fisher, Marin Soljacic, "Wireless Power Transfer via Strongly Coupled Magnetic Resonances," *Science Magazine*, Vol.317, No.5834, pp.83-86, 2007.
- [2] Arsteidis Karalis, J. D. Joannopoulos, Marin Soljacic, "Efficient wireless non-radiative mid-range energy transfer," *Annals of Physics*, Vol. 323. No. 1, pp. 34-48, Jan. 2008.
- [3] Hiroshi Hirayama, Toshiyuki Ozawa, Yosuke Hiraiwa, Nobuyoshi Kikuma, Kunio Sakakibara, "A Consideration of Electromagnetic- resonant Coupling Mode in Wireless Power Transmission," *IEICE ELEX*, Vol. 6, No. 19, pp. 1421-1425, Oct. 2009
- [4] Hiroshi Hirayama, Nobuyoshi Kikuma, Kunio Sakakibara, "An consideration on equivalent circuit of wireless power transmission," *Proc. of Antennas*, Jul. 2010
- [5] Hiroshi Hirayama, Nobuyoshi Kikuma, Kunio Sakakibara, "Undesired emission from Magnetic-resonant wireless power transfer," *Proc. of EMC Europe*, Sep. 2010
- [6] I. Awai, "Design Theory of Wireless Power Transfer System Based on Magnetically Coupled Resonators," *Proc. 2010 IEEE International Conference on Wireless Information Technology and Systems*, Aug. 2010.
- [7] Qiaowei Yuan, Qiang Chen, Kunio Sawaya, "Transmission Efficiency of Evanescent Resonant Coupling Wireless Power Transfer System with Consideration of Human Body Effect," *IEICE Tech. Report*, vol. 108, no. 201, AP2008-91, pp. 95-100, Sep. 2008.
- [8] Koichi Tsunekawa, "A Feasibility Study of Wireless Power Transmission using Antenna Mutual Coupling Technique on Indoor Ubiquitous Wireless Access System," *IEICE Tech. Report*, vol. 108, no. 304, AP2008-113, pp. 13-18, Nov. 2008.
- [9] Masato Tanaka, Naoki Inagaki, Katsuyuki Fujii, "A new wireless connection system through inductive magnetic field," *IEICE Tech. Report*, vol. 108, no. 386, AP2008-184, pp. 197-202, Jan. 2009.



Wireless Power Transfer - Principles and Engineering Explorations

Edited by Dr. Ki Young Kim

ISBN 978-953-307-874-8

Hard cover, 272 pages

Publisher InTech

Published online 25, January, 2012

Published in print edition January, 2012

The title of this book, *Wireless Power Transfer: Principles and Engineering Explorations*, encompasses theory and engineering technology, which are of interest for diverse classes of wireless power transfer. This book is a collection of contemporary research and developments in the area of wireless power transfer technology. It consists of 13 chapters that focus on interesting topics of wireless power links, and several system issues in which analytical methodologies, numerical simulation techniques, measurement techniques and methods, and applicable examples are investigated.

How to reference

In order to correctly reference this scholarly work, feel free to copy and paste the following:

Hiroshi Hirayama (2012). Equivalent Circuit and Calculation of Its Parameters of Magnetic-Coupled-Resonant Wireless Power Transfer, *Wireless Power Transfer - Principles and Engineering Explorations*, Dr. Ki Young Kim (Ed.), ISBN: 978-953-307-874-8, InTech, Available from: <http://www.intechopen.com/books/wireless-power-transfer-principles-and-engineering-explorations/equivalent-circuit-and-calculation-of-its-parameters-of-magnetic-coupled-resonant-wireless-power-tra>

INTECH

open science | open minds

InTech Europe

University Campus STeP Ri
Slavka Krautzeka 83/A
51000 Rijeka, Croatia
Phone: +385 (51) 770 447
Fax: +385 (51) 686 166
www.intechopen.com

InTech China

Unit 405, Office Block, Hotel Equatorial Shanghai
No.65, Yan An Road (West), Shanghai, 200040, China
中国上海市延安西路65号上海国际贵都大饭店办公楼405单元
Phone: +86-21-62489820
Fax: +86-21-62489821

© 2012 The Author(s). Licensee IntechOpen. This is an open access article distributed under the terms of the [Creative Commons Attribution 3.0 License](#), which permits unrestricted use, distribution, and reproduction in any medium, provided the original work is properly cited.